Nonlinear Analysis: Modelling and Control, Vol. 30, No. 3, 483–498
https://doi.org/10.15388/namc.2025.30.39328

Vilnius University Press

Control of the servo motor using feedback linearization and artificial gorilla troops optimizer*

Radiša Jovanović, Mitra Vesović

Faculty of Mechanical Engineering of the University of Belgrade,
Kraljice Marije 16, 11120, Belgrade, Serbia
rjovanovic@mas.bg.ac.rs; mvesovic@mas.bg.ac.rs

Received: March 2, 2023 / **Revised:** February 25, 2025 / **Published online:** March 10, 2025

Abstract. This paper establishes a nonlinear optimization strategy for position control of a direct current motor. When experimental evidence showed that the linear model does not sufficiently represent the system, the model is modified from linear to nonlinear, using friction-induced nonlinearity. In the course of the research, an analysis of the nonlinear feedback linearizing controller and the up to date gorilla troops optimization algorithm are carried out. The proposed algorithm is juxtapose with four others metaheuristic optimizations. Furthermore, performances with and without different types of disturbances are compared for individual desired output signals. The experimental results corroborate the nonlinear control's robustness.

Keywords: nonlinear modelling, artificial gorilla troops optimizer, African vultures optimization algorithm, feedback linearization approach, stochastic disturbance robustness.

1 Introduction

A variety of methods may be used to regulate the position of the output series direct current (DC) motor shaft. Traditional feedback control systems are commonly used, such as proportional-integral-derivative (PID-like) controllers. They are simple and affordable (in comparison to more complicated control systems), and many versions of these control systems manage to keep the system's output well matched with the specified value within error limits. They, on the other hand, are unable to withstand adversity [17].

Aside from basic controllers, there are a variety of nonlinear controllers available [24]. In [16], a brand-new adaptive approach is created for controlling DC motors. In this approach, the plant is controlled concurrently using PID and artificial neural networks (ANN). The neural network feed forward controller is trained using the PID controller. For the same issue, however, paper [15] proposes the design of a fuzzy logic controller (FLC). Global optimization problems are difficult to solve efficiently because of their

*The paper is a part of the research done within the project supported by the Ministry of Science, Technological Development and Innovation of the Serbian Government RS under contract 451-03-137/2025-03/ 200105 from 04.02.2025.

significant nonlinearity and multiple local optima. With nonlinear equations, however, the individual equilibrium stability must be verified [9].

Nature has been a major source of inspiration in this subject. These methods include popular algorithms such as: the firefly algorithm (FA) [23], the particle swarm algorithm (PSO) [5], the differential evolution (DE) algorithm [18], the genetic algorithm (GA) [8]; some recently developed algorithms: the grey wolf optimization (GWO) [13] and the whale optimization algorithm (WOA) [12]; some newly discovered algorithms: the artificial gorilla troops optimizer (GTO) [2] and the African vultures optimization algorithm (AVOA) [1] and many others. These algorithms have found wide application. For example, [3] and [7] use GTO for tuning the control system parameters. Supplemental nonlinear control methods can be used in combination with other tactics.

For example, feedback linearization (FBL) permits the production of linear control law through the synergy of a nonlinear transformation and linearization with feedback loop, by canceling the nonlinearities in the system model. This method has shown to be useful in a wide range of control tasks, including robotic systems, high-performance aircraft, helicopters, biomedical equipment, and general industries [9], or it can be used as position controller for DC motor [21]. This nonlinear technique can be combined with metaheuristics optimization in order to obtain controller that will provide best machine performance [10, 19, 22].

As the continuation of the research [20], the FBL approach was also utilized in this study. It was carried out using a mathematical model that accounts for friction-induced nonlinearity. Unlike past research on related subjects, that construct the model in compliance with the flux and motor current nonlinearities [4, 11, 14], here a unique model with discontinuous nonlinearity was developed utilizing the Tustin model and Stribeck friction. This model was approximated by a differentiable function of the hyperbolic tangent. In this way, all of the constraints and all of the requirements for FBL application are met. After fully utilizing the FBL strategy to algebraically reduce the system's nonlinearities to their linear forms, the innovative GTO optimization method, as recent metaheuristics intelligence methodology, was used to solve the challenge of determining controller coefficients. Furthermore, in order to juxtapose this method, the comparison is made with the AVOA, GWO, WOA and FA.

The last contribution of the research is an experimental demonstration of the robustness and effectiveness of nonlinear system control in the face of both, continuous and pulse disruption in the form of the white noise and external step disturbances acting up on the object.

2 Object description

All systems, including mechanical ones, are mostly very complex and nonlinear. When there are simpler models, for example linear ones, there is no need to work with more complicated. However, neglecting nonlinearities in some cases significantly affects the design of the control system. On the other hand, accurate mathematical models are tough to obtain. A schematic depiction of a series wounded DC motor is shown in Fig. 1.

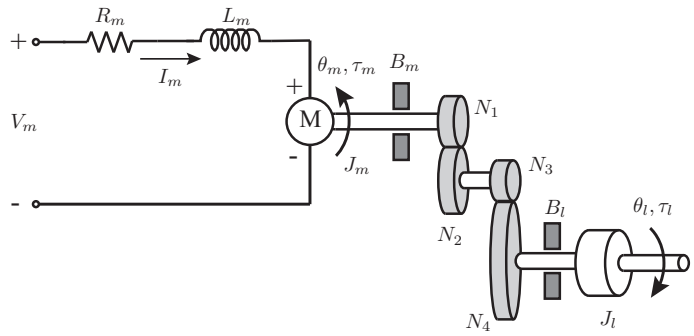

Figure 1. The armature circuit and gain train for the SRV02 DC motor [6].

Figure 1 shows a schematic representation of a series-wound DC motor, with V_m standing for voltage, R_m for resistance, I_m for current, and L_m for the motor's inductance. Load moment of inertia is represented by J_l, motor shaft moment of inertia by J_m, motor shaft position by θ_m, load shaft position by θ_l, viscous friction acting on the motor shaft B_m and load shaft B_l. Total torque applied on the load is τ_l and on the motor is τ_m. N_i, $i = 1, 2, 3, 4$, are gears. To address the challenges identified, this paper begins by describing the DC motor's structural and operational characteristics, emphasizing the nonlinearities that inform the subsequent control strategy.

2.1 Selection of a mathematical model

Given the complex nature of the DC motor, an accurate mathematical model is essential for developing robust control strategies. In this section, a model that captures dynamics and incorporating friction-induced nonlinearities is presented. Using motor voltage as an input variable $V_m = u$, the position of the load shaft $\theta_l = y$ as an output variable and including the total moment of inertia J_{eq}, the equivalent damping term $B_{eq,v}$, and the actuator gain A_m, the linear model for the system is:

$$J_{eq}\ddot{y}(t) + B_{eq,v}\dot{y}(t) = A_m u(t)$$

The numerical values of the object's parameters are given in Section 5. The speed-dependent friction nonlinearity was used to build the DC motor's nonlinear mathematical model. Many friction models differ largely in how they characterize the moment of friction, which has been thoroughly investigated in the literature. In these approaches the friction torque is expressed as a static and/or dynamic function of rotational velocity. In this research, the Tustin friction model was employed [6]:

$$\begin{aligned} T_{fric} &= T_{visc} + T_{st} \\ &= T_c \operatorname{sgn}(\dot{\theta}_l) + (T_s - T_c)\mathrm{e}^{\dot{\theta}_l/\dot{\theta}_s} \operatorname{sgn}(\dot{\theta}_l) + B\dot{\theta}_l, \end{aligned}$$

T_{visc} is viscous friction part, T_{st} is Stribeck function with an upper bound equal to the static friction torque T_s at zero velocity and a lower bound equal to the Coulomb friction

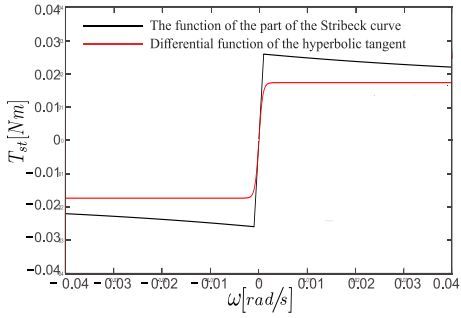

Figure 2. Approximation of the part of the friction curve [21].

torque T_c. This is a decreasing function as Stribeck velocity $\dot{\theta}_s$ increases. B is the viscous friction coefficient. As a result, a nonlinear mathematical model is used as

$$J_{eq}\ddot{y}(t) + T_{st}\big(\dot{y}(t)\big) + B_{eq,n}\dot{y}(t) = A_m u(t),$$

where T_{st} is the nonlinear segment of the friction torque (Stribeck), $B_{eq,n}$ is the equivalent damping term in which the linear viscous friction is already comprehended. Because the Stribeck effect is most noticeable at low velocities, the portion of the derived friction curve $T_{st}(\dot{\theta}_l)$ at velocities between -0.04 and 0.04 rad/s is shown in Fig. 2. For negative and positive values of angular velocity, friction properties are considered to be symmetrical. The approximation is performed using the tangent hyperbolic function: $f(\dot{\theta}_l) = \lambda_1(2/(1+\mathrm{e}-\lambda_2\dot{\theta}_l)-1)$, where λ_1 and λ_2 are numerical constants with values given in Section 5. In order to avoid the jump discontinuity of the recommended friction model and since the FBL technique requires differentiable functions (as will be seen in the subsequent section) the exponential component of the Stribeck curve (static friction) is neglected, and only Coulomb and viscous friction are described in this way [21]. The state equation of the system can be written as Eq. (1). State variables are given as: $x_1 = \theta_l$ and $x_2 = \dot{\theta}_l$.

$$\dot{\boldsymbol{x}} = \begin{bmatrix}\dot{x}_1\\ \dot{x}_2\end{bmatrix} = \begin{bmatrix}0 & 1\\ 0 & -\frac{B_{eq,n}}{J_{eq}}\end{bmatrix}\boldsymbol{x} + \begin{bmatrix}0\\ -1\end{bmatrix} f(\boldsymbol{x}) + \begin{bmatrix}0\\ \frac{A_m}{J_{eq}}\end{bmatrix} u, \qquad y = \begin{bmatrix}1 & 0\end{bmatrix}\boldsymbol{x}. \tag{1}$$

2.2 Verification of the mathematical model

Having established a mathematical model, its validity is assessed through a comparison with empirical data, as detailed in the provided section. Comparisons were made between the responses produced from the linear and nonlinear models for step and sinusoidal inputs, Fig. 3. The responses of the real object and the linear model to step and sinusoidal excitations do not match well. For the step input, the model does not accurately reflect the system's real behavior. To construct the most realistic model of a DC motor and to allow a fair synthesis of the control system subsequently, the nonlinearity of friction must be studied and taken into account.

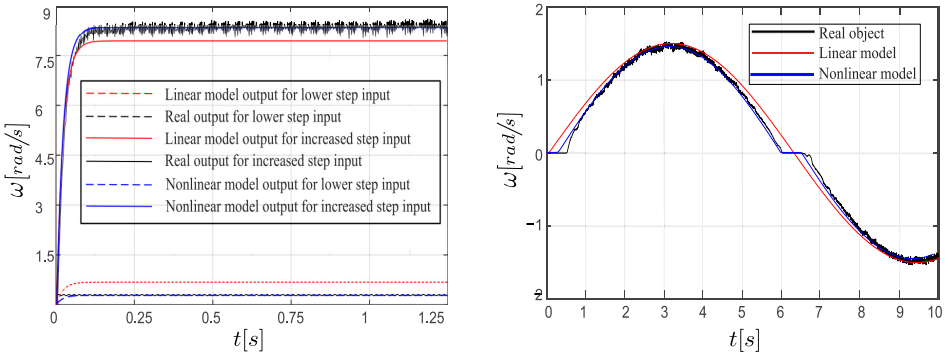

Figure 3. Actual behavior and two models.

3 Feedback linearization limitations

3.1 A brief overview of the method

The theoretical groundwork for executing the proposed FBL approach will be discussed in this part in order to algebraically eliminate nonlinearities from the system. The idea of nonlinear cancellation is conceptually general and theoretically robust but practically constrained by the specific characteristics of the system being controlled. It is best suited for systems where the nonlinearities can be modeled accurately and satisfy the mathematical conditions necessary for cancellation. When these conditions are not met, alternative strategies like adaptive, robust, or hybrid control methods are often employe. Clearly, we should not expect to be able to cancel nonlinearities in every nonlinear system. There must be a certain structural property of the system that allows as to prefer such cancellation [9].

Examine the nonlinear system class

$$\begin{aligned}\dot{\mathbf{x}} &= \mathbf{f}(\mathbf{x}) + \mathbf{g}(\mathbf{x})\mathbf{u},\\ y &= h(\mathbf{x})\end{aligned}$$

where $\mathbf{f}(\mathbf{x})$, $\mathbf{g}(\mathbf{x})$ and $h(\mathbf{x})$ are sufficiently smooth in a domain $D \subset \mathbb{R}^n$, $\dot{\mathbf{x}} = [x_1, x_2, x_3, \ldots, x_n]^{\mathrm{T}}$ is a state vector and $\mathbf{u}$ is the state feedback control. It is undeniable that this concept cannot always be generalized; cancellation must be permitted by unique systemic characteristics. In order to accomplish this type of control, four requirements must be met.

- In the first place, the system's state equation must have the following form:

$$\dot{\mathbf{x}} = A\mathbf{x} + B\gamma(\mathbf{x})\big[u - \alpha(\mathbf{x})\big],$$

where A is $n \times n$ and B is $n \times p$ matrix. The function $\alpha : \mathbb{R}^n \to \mathbb{R}^p$ and $\gamma : \mathbb{R}^n \to \mathbb{R}^{p \cdot p}$ are defined on domain that contains the origin and reflect possible nonlinearities in the system. It is not difficult to remark that to cancel a nonlinear component $\alpha(\mathbf{x})$ by subtraction, the control signal $\mathbf{u}$ and the nonlinearity $\alpha(\mathbf{x})$ must

appear together as the sum: $\mathbf{u} + \alpha(\mathbf{x})$. On the other hand, to undo the nonlinear component $\gamma(\mathbf{x})$ by division, the control $\mathbf{u}$ and nonlinearity $\gamma(\mathbf{x})$ must always appear as a product $\gamma(\mathbf{x})\mathbf{u}$. If the square matrix $\gamma(\mathbf{x})$ is nonsingular in the domain of interest, then it can be cancelled by $u = \beta(\mathbf{x})\mathbf{v}$, where $\beta(\mathbf{x}) = \gamma^{-1}(\mathbf{x})$ is the inverse of the matrix $\gamma(\mathbf{x})$.

- $\gamma(\mathbf{x})$ has to be nonsingular for any $\mathbf{x}$ in the domain of interest $\mathbf{x} \in D$ or if it is a scalar value then it has to be nonzero value.
- The controllability of the pair $(\mathbf{A}, \mathbf{B})$ is required.
- All functions must be differentiable.

The satisfied control law, which yields a new control signal $\mathbf{v}$, can be produced under these conditions as follows: $\mathbf{u} = \alpha(\mathbf{x}) + \gamma^{-1}(\mathbf{x})\mathbf{v}$ [9].

3.1.1 Input-output feedback linearization

Even though one component of the state equation remains nonlinear, it is sometimes more cost-effective to do linearization simply from input to output. It is required to know the system's relative degree in order to assess whether linearization of all states is conceivable or whether internal dynamics exist. Input-Output Feedback can be performed when the system's relative degree equals the order of the system, because only then full state linearization is possible. In Eq. (2), r represents the relative degree of the system (the number of output signal derivatives required to determine the input's explicit dependency), L denotes Lie derivatives of the functions $\mathbf{f}$ and $\mathbf{g}$ from the nonlinear system class: $\dot{\mathbf{x}} = \mathbf{f}(\mathbf{x}) + \mathbf{g}(\mathbf{x})u$ and $y = h(\mathbf{x})$. The system is linearized through feedback from input to output by using the following u:

$$y^r = L_{\mathbf{f}}^r h(\boldsymbol{x}) + L_{\mathbf{g}} L_{\mathbf{f}}^{r-1} h(\boldsymbol{x})u, \quad u = \frac{1}{L_{\mathbf{g}} L_{\mathbf{f}}^{r-1} h(\boldsymbol{x})}\big(-L_{\mathbf{f}}^r h(\boldsymbol{x}) + v\big). \tag{2}$$

3.2 Fulfillment of conditions

Applying constraints of the FBL from the previous Section to the system equation (1) yields

$$A = \begin{bmatrix} 0 & 1 \\ 0 & -\frac{B_{eq,n}}{J_{eq}} \end{bmatrix}, \qquad B = \begin{bmatrix} 0 \\ \frac{A_m}{J_{eq}} \end{bmatrix}, \qquad \alpha(\boldsymbol{x}) = \frac{J_{eq}}{A_m} f(\boldsymbol{x}), \qquad \gamma(\boldsymbol{x}) = 1.$$

Firstly, in this paper, no transformation of the system is needed because the state equation does have the desirable structure for already accepted choice of state variables. Since the system is already in the right shape for FBL, coordinate transformation is not required.

In this model, $\gamma(\mathbf{x})$ appears explicitly in the system's state-space representation. As it is already mentioned, generally, to cancel nonlinear $\gamma(\mathbf{x})$ term, the control u and the nonlinearity $\gamma(\mathbf{x})$ must always appear as a product $\gamma(\mathbf{x})u$. If the $\gamma(\mathbf{x})$ is matrix and nonsingular in the domain of interest than it can be cancelled by the inversion. If it is

a scalar value then it has to be nonzero value. For the given system, it is defined as scalar, $\gamma(\mathbf{x}) = 1$. This simplification arises because in a given system there are no nonlinearities that multiply with the control signal. As a result, $\gamma(\mathbf{x})$ being unity ensures that it is nonzero for all $\mathbf{x}$, thus inherently satisfying the nonsingularity condition. This specific characteristic of the model greatly simplifies the discussion, as no additional analysis is required to verify the invertibility of $\gamma(\mathbf{x})$. In practical terms, it eliminates the need to account for singularities, which might otherwise arise in systems with more complex forms. From the above discussion it follows that the second criterion is also met because $\gamma(\mathbf{x})$ is nonzero value.

Furthermore, the controllability matrix is $U = [B \;\; AB \;\; A^2B \;\; \cdots \;\; A^{n-1}B]$. Since order of the system is $n = 2$, the controllability matrix evaluates to

$$U = [B \;\; AB] = U = \begin{bmatrix} 0 & \frac{A_m}{J_{eq}} \\ \frac{A_m}{J_{eq}} & -\frac{B_{eq,n}A_m}{J_{eq}^2} \end{bmatrix}.$$

Because this matrix is full rank, $\operatorname{rank} U = n = 2$, the pair (A, B) is controllable. The number of the noncontrollable states is equal to the zero. It can easily be concluded that applying constraints of the FBL to the system in this paper, the controllability of (A, B) hinges on the values of A_m and $B_{eq,n}$. Since these parameters represent physical properties (actuator gain and damping, respectively) and are nonzero in practical systems, the controllability condition is inherently satisfied.

Finally, since the approximation using the differentiable tangent hyperbolic was achieved before, all functions are smooth and differentiable.

Since the system output's first derivative is independent of the control signal, the system's relative degree is not 1. The relative degree of this system is equal to the system order r = 2. The control signal u can be chosen in the following form:

$$\begin{aligned} u &= \frac{1}{L_{\mathbf{g}}L_{\mathbf{f}}h(x)}\left(-L_{\mathbf{f}}^2h(x) + v\right) = \frac{J_{eq}}{A_m}\left[\frac{B_{eq,n}}{J_{eq}}x_2 + f(x) + v\right], \\ v &= -K_0x_1 - K_1x_2 + K_2x_{ref}. \end{aligned} \tag{3}$$

Thus, all conditions for feedback linearization are satisfied, as explicitly demonstrated. Feedback linearization, while powerful, requires parameter tuning. This challenge is addressed using GTO, as explained below.

4 Optimization of the nonlinear controller

A metaheuristic algorithm is a search process meant to discover a decent solution to a complex and difficult to solve optimization problem. In this study, GTO is used to optimize the controller parameters. In addition, four different metaheuristic techniques are used for comparison: the WOA, GWO, AVOA and FA. The general task of optimization in metaheuristic algorithms is to find the best solution (or a near-optimal one) to a given problem within a feasible search space, where traditional optimization methods may fail due to complexity, nonlinearity, or the presence of multiple local optima. In the context

of optimization, the task of a metaheuristic algorithm is to minimize (or maximize) an objective function that measures the quality of a solution. The algorithm aims to find the best possible solution within the defined search space, ensuring that it outperforms or matches all other potential solutions, while also satisfying any specific constraints of the problem. Metaheuristic algorithms are designed to efficiently explore and exploit the search space, balancing between global and local search capabilities.

4.1 Artificial gorilla troops optimizer

The GTO algorithm employs five separate operators based on gorilla behaviours. In the exploration phase, three distinct operators were used: migration to an unfamiliar location to boost GTO exploration; a move to the other gorillas to raise the level of exploration and exploitation and migration towards a known place, which considerably enhances the GTO's power to explore for alternative optimization spaces. In the exploitations phase, two operators are employed, which considerably improves the search performance. This algorithm was proposed for the first time in [2], and a brief mathematical description of this algorithm is given below.

4.1.1 Exploration phase

All gorillas are considered candidate solutions in the GTO algorithm and the best candidate solution at each optimization operation step is referred to as a silverback gorilla. The first mechanism, technique of migration to an unknown location, is chosen using a parameter named p, namely, if $rand$ is less than p. Parameter p represents the probability of selecting the migration to an unknown location mechanism during the exploration phase. It governs the balance between exploration (searching new areas) and exploitation (refining existing solutions). It decides which exploration mechanism is applied based on a randomly generated value $rand$. However, the technique of migration towards other gorillas is selected if $rand$ is greater or equal than 0.5. Finally, for $rand$ is less than 0.5 the technique of migration to a known location is chosen. The three processes were simulated using Eq. (4), where $GX(t+1)$ is the candidate position vector containing the optimization parameters (K_0, K_1, K_2) in the next t iteration and $X(t)$ is the current vector, i.e., part of the optimization process to determine the optimal control parameters (K_0, K_1, K_2) for feedback linearization. Moreover, r_1, r_2, r_3, and $rand$ are random values ranging from 0 to 1 updated in each iteration, and p determines the probability of selecting the migration mechanism to an unknown location.

$$GX(t+1) = \begin{cases} (UB - LB) \cdot r_1 + LB, & rand < p, \\ (r_2 - C) \cdot X_r(t) + L \cdot H, & rand \geqslant 0.5, \\ X(i) - L \cdot (L \cdot X(t) - GX_r(t)) & \\ \quad + r_3 \cdot (X(t) - GX_r(t)), & rand < 0.5, \end{cases} \tag{4}$$

UB and LB represent the upper and lower bounds of the variables, respectively. X_r is one member of the gorillas in the group randomly selected from the entire population

and also GX_r is one of the vectors of gorilla candidate positions randomly selected but includes the positions updated in each phase. Finally, C, and L are calculated as: $C = F \cdot (1 - It/MaxIt)$, $F = \cos(2r_4) + 1$ and $L = C \cdot l$. Here It is the current iteration value, and $MaxIt$ is the maximum number of iterations. l is a number between -1 and 1 that is as well chosen at random. Also, in Eq. (4), H is as $H = Z \cdot X(t)$, while Z is calculated using $Z = [-C\ C]$. A group formation operation is carried out at the end of the exploration phase and at the conclusion the cost of all GX solutions is computed. If the cost of the $GX(t)$ is smaller than cost of the $X(t)$, $f(GX(t)) < f(X(t))$, the $GX(t)$ solution is utilized as the $X(t)$ solution. As a result, the best solution created during this phase is referred to as a silverback. Having established the exploration mechanisms of the GTO, we next detail its exploitation strategies, critical for fine-tuning the solution space.

4.1.2 Exploitation phase

Using the C value one of the two behaviors, follow the silverback or competition for adult females equations (5) and (6), can be selected during the exploitation phase of the GTO algorithm. W serves as a threshold for determining which behavior is used during the exploitation phase: follow the silverback or competition for adult females. It controls the shift from cooperative to competitive dynamics as the algorithm progresses. W is compared with the computed value C in the exploitation phase: If $C \geqslant W$ is selected, the silverback mechanism is used, however if $C < W$ is selected, adult females' competition is selected. The first type of behavior, the silverback is described with Eq. (5), where $X(t)$ is the gorilla position vector and $X_{silverback}$ is the silverback gorilla position vector, i.e., best solution. $GX_i(t)$ represents the vector location of each potential candidate in iteration t. The total number of gorillas is denoted by the letter N. Equation (6) is used to simulate the second type of behaviour-competition.

$$\begin{aligned} GX(t+1) &= L \cdot M \cdot \big(X(t) - X_{silverback}\big) + X(t), \\ M &= \left(\left| \frac{1}{N} \sum_{i=1}^{N} GX_i(t) \right|^g \right)^{1/g}, \quad g = 2^L. \end{aligned} \tag{5}$$

$$\begin{aligned} GX(i) &= X_{silverback} - \big(X_{silverback} \cdot Q - X(t) \cdot Q\big) \cdot A, \\ E &= \begin{cases} N_1, & rand \geqslant 0.5, \\ N_2, & rand < 0.5. \end{cases} \end{aligned} \tag{6}$$

Here, $Q = 2r_5 - 1$ is used to mimic the impact force, while r_5 and $rand$ are random numbers between 0 and 1. The coefficient vector $A = \beta \cdot E$ is used to determine the degree of violence in conflicts. Value E uses a threshold of 0.5 to simulate how violence impacts the limits of solutions and β determines the degree of intensity in conflicts during the competition for adult females phase of the GTO algorithm, influencing how aggressively candidate solutions compete for improvement. The cost of all GX solutions is evaluated at the end and if the cost of $GX(t)$ is smaller than the cost of the $X(t)$, $f(GX(t)) < f(X(t))$ the $GX(t)$ solution is utilized as the $X(t)$ solution, and the best solution produced among the whole population is seen as a silverback.

4.2 Metaheuristic optimization algorithms for comparison

The GTO results are compared to the four distinct optimization algorithms: the GWO, WOA, AVOA, and FA. The default values are set for all of the parameters.

Seyedali Mirjalili et al. presented the GWO as a revolutionary heuristic intelligence optimization technique in [13].

The WOA [12] is a metaheuristic algorithm based on humpback whales' hunting strategy, which involves swimming up to the surface while producing bubbles in a spiral form around the target.

The AVOA is very recent algorithm based on African vulture hunting behaviour [1].

The FA [23], is another population-based optimization approach, which has been challenged for only having a little difference from the well-known particle swarm optimization.

4.3 Optimization of FBL controller using the artificial gorilla troop algorithm

K_0, K_1 and K_2 from Eq. (3) are three parameters in the proposed FBL controller that may be modified to produce the optimal dynamical response. This study's exclusive focus has been on the modification of these gains. Moreover, to design the optimal FBL controller, the GTO optimization approach was used. In addition, each of the aforementioned parameters is programmed into a single agent, which in our situation is given a vector with three parameters. All of the optimization processes find optimal controller gains in a discrete framework. Those fixed gains are then applied in the real-time continuous system. The optimization algorithm is executed offline, before real-time control is implemented. The DC motor operates smoothly due to set optimal gains and no dynamic gain swapping.

The objective function performance requirements employ the integral of time-weighted absolute error (ITAE) performance criteria:

$$\mathrm{ITAE} = \int_0^{t_f=10} t\big|\varepsilon(t)\big|\,\mathrm{d}t,$$

where $\varepsilon(t) = y_d(t) - y(t)$ represents the difference between the desired output y_d and the real output - the position of the load shaft.

The maximum number of iterations and the number of search agents are both fixed at 50 and 30 respectively. Furthermore, a single agent represents one potential ideal controller. GTO was compared against four other optimization algorithms in the experimental section: the AVOA, WOA, GWO, and FA. The parameters of all algorithms are taken from original papers [1, 2, 12, 13] and [23], respectively. Due to a fair comparison, all of the algorithms have the same goal function, a number of iterations, and search agents.

To validate the optimized controller parameters derived through the proposed metaheuristic approach, extensive experiments were conducted, as detailed below.

5 Experimental results

The numerical values of the object's parameters are: $J_{eq} = 0.0021$ kg m^2, $B_{eq,v} = 0.0840$ Nm/rad/s, $B_{eq,n} = 0.0721$ Nm/rad/s, $A_m = 0.1284$ Nm/V, $\lambda_1 = 0.0173607$, and $\lambda_2 = 2500$. The results of applying the various optimization methodologies to the proposed control are summarized.

The results are averaged over 50 independent runs, and all of the algorithms give similar results with ITAE, shown in Table 1. The best results are indicated in the bold type.

The convergence curve of the objective function value is depicted in Fig. 4. From Table 1 and Fig. 4 it is possible to conclude that, according to minimal value of the objective function, GTO and AVOA gave better results comparing to GWO, WOA and FA, but the best result is obtained by GTO. Despite the fact that all of the outcomes are comparable, gorillas continue to perform the best. As a consequence, the following results are solely for GTO.

With $K_0 = 442.72$, $K_1 = 442.75$ and $K_2 = 30$, efficiency of proposed optimized FBL controller is tested for the ensuing cases.

First of all, desired trajectories are defined as constant value and sinusoidal signal.

In the first case, the output and intended trajectory signals are fairly similar, with slight differences. It is evident from Fig. 5(a), which shows position tracking for a constant value signal $2\pi/3$, that the system reacts fast.

With an overshoot less than 3.5% and a steady state error of 0.015, the rising and settling times are both less than 0.39 seconds.

Sinusoidal signals, in which the output shaft rotates in a different direction throughout operation, are also particularly useful for evaluating the performance of a nonlinear control system.

As a result, Fig. 5(b) shows a sinusoidal signal with amplitude 2 and frequency 1 Hz.

In the second case, the study is expanded to examine the robustness of the controller.

The white noise disturbance is introduced as a more generic scenario, which is an important measurement when examining the robustness of the control algorithms. White noise is introduced as a method of simulating random excitation. This is a random process with a constant power spectral density.

To demonstrate the efficiency of the suggested optimization, simulations with a band-limited white noise introduced to the controlled variable and experimental findings on a laboratory plant are employed.

Table 1

Optimization algorithm	Objective function: average value	Objective function: the best value
FA	0.1035	0.0767
GWO	0.0883	0.0824
WOA	0.0854	0.0837
AVOA	0.0810	0.0757
GTO	**0.0804**	**0.0753**

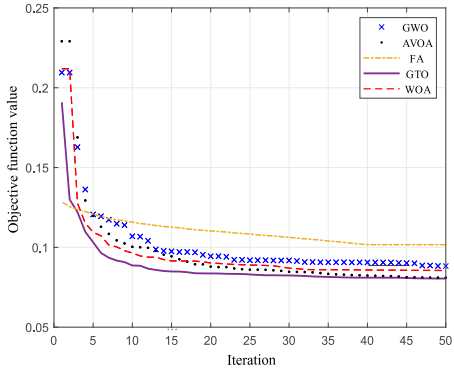

Figure 4. The convergence curve of the ITAE

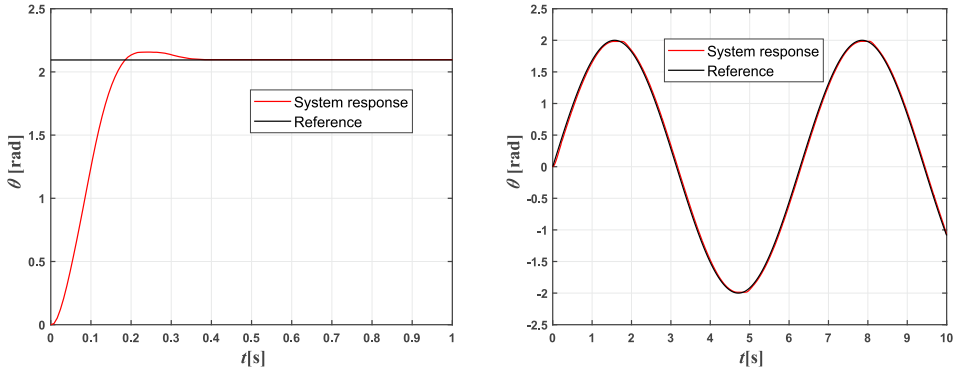

Figure 5. Position tracking for constant (a) and sinusoidal signal (b) as desired output signals.

Although the suggested controller's coefficients are tuned for the disturbance-free situation, the responses are strikingly similar to the first instance. The difference is practically imperceptible graphically, so Fig. 6 shows the error signal for the position tracking for reference signal: $x_{ref} = 2\pi/3$.

Finally, in the third instance, a disturbance that occurs between the third and fourth second is applied. The disturbance d is simulated using two time-delayed unit step functions, shown on Fig. 6(b). Figure 7(a) shows minor deviations from the desired output between the third and fourth second. In that time interval, the error is less than 0.057 rad.

After the disturbance has ceased, the system needs about 0.014 seconds to return to steady state.

Since the intensity of the disturbance is equal to the intensity of the desired output signal, it can be considered that the control system manages to cause the object to follow the given desired output signal.

Figure 7(a) shows good tracking of the given signal, without any major deviations.

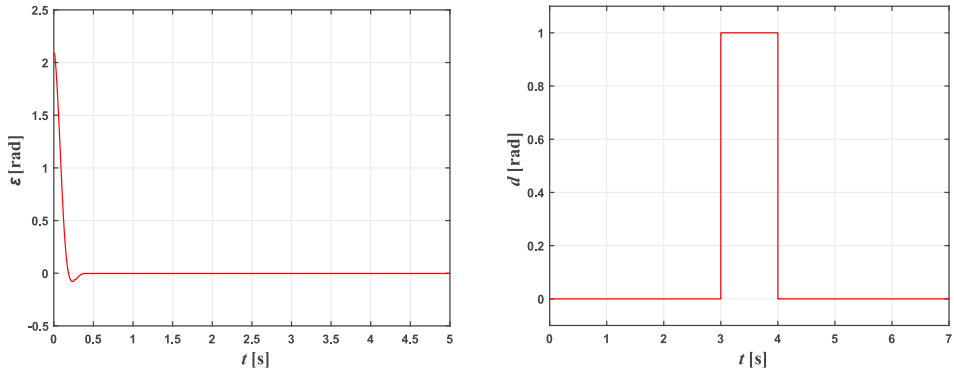

(a) (b)

Figure 6. Tracking error for constant value with white noise applied as disturbance (a). Case 3: Disturbance acting on the object (b).

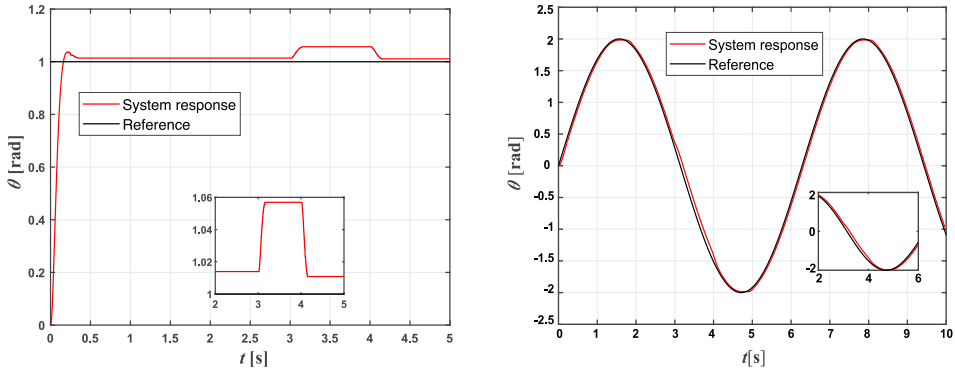

(a) (b)

Figure 7. Position tracking with descrete disturbance for unit step (a) and sinusoidal signal (b).

The experimental results demonstrate the proposed controller's robustness and precision, affirming its potential as a practical solution, as summarized in the conclusion.

6 Conclusion

This study is an extension of the study [20], in which the position of the load shaft of a DC motor is regulated using the FBL technique, whose gains were optimized using the GWO algorithm. Friction modeling using the Tustin, i.e., Stribeck model resulted in a nonlinear mathematical model of the object. The hyperbolic tangent was discovered as an approximation of a section of the Stribeck friction curve and was utilized as the nonlinearity function. Following that, the requirements for correctly implementing FBL, as well as the theory of the GTO technique, were investigated. This approach has been

used to consider the prerequisites for synthesis of the control law. Finally, gains for the proposed FBL controller were obtained using the GTO optimization approach. To compare its performance, four other algorithms: the AVOA, GWO, WOA, and FA are used. It was demonstrated that GTO had the lowest objective function, making it preferable than the others. Proposed controller was capable of dealing with the nonlinearities of the DC motor. Further, two types of disturbances were introduced to test the robustness. As the suggested technique works over a wide range of outputs and because the desired and actual trajectory are so similar in all of the situations studied, it is feasible to infer that the proposed optimal feedback linearizing controller provides a viable solution to the stated problem.

References

1. B. Abdollahzadeh, F.S. Gharehchopogh, S. Mirjalili, African vultures optimization algorithm: A new nature-inspired metaheuristic algorithm for global optimization problems, *Comput. Ind. Eng.*, **158**:107408, 2021, https://doi.org/10.1016/j.cie.2021.107408.
2. B. Abdollahzadeh, F.S. Gharehchopogh, S. Mirjalili, Artificial gorilla troops optimizer: A new nature-inspired metaheuristic algorithm for global optimization problems, *Int. J. Intell. Syst.*, **36**(10):5887–5958, 2021, https://doi.org/10.1002/int.22535.
3. M. Ali, H. Kotb, K. M. Aboras, N. H. Abbasy, Design of cascaded PI-fractional order PID controller for improving the frequency response of hybrid microgrid system using gorilla troops optimizer, *IEEE Access*, **9**:150715–150732, 2021, https://doi.org/10.1109/ACCESS.2021.3125317.
4. M. Boroujeni, GR Arab Markadeh, J. Soltani, Torque ripple reduction of brushless DC motor based on adaptive input-output feedback linearization, *ISA Trans.*, **70**:502–511, 2017, https://doi.org/10.1016/j.isatra.2017.05.006.
5. R. Eberhart, J. Kennedy, A new optimizer using particle swarm theory, in T. Fukuda (Ed.), *MHS'95. Proceedings of the Sixth International Symposium on Micro Machine and Human Science, Nagoya Municipal Industrial Research Institute, October 4–6, 1995*, IEEE, Piscataway, NJ, 1995, pp. 39–43, https://doi.org/10.1109/MHS.1995.494215.
6. L.T. Gruyitch, Z. Bučevac, R. Jovanović, Z.B. Ribar, Structurally variable control of Lurie systems, *Int. J. Control*, **93**(12):2960–2972, 2019, https://doi.org/10.1080/00207179.2019.1569764.
7. M.K. Gude, U. Salma, Artificial gorilla troops optimizer for tuning power system stabilizer control parameters, in *2021 IEEE 2nd International Conference On Electrical Power and Energy Systems (ICEPES), Bhopal, India, 10–11 December, 2021*, IEEE, Piscataway, NJ, 2021, pp. 1–5, https://doi.org/10.1109/ICEPES52894.2021.9699780.
8. J. Holland, *Adaptation in Natural and Artificial Systems*, Univ. Michigan Press, Michigan, 1992.
9. H. Khalil, *Nonlinear Systems,* 3rd ed., Prentice-Hall, Upper Saddle River, NJ, 2002.
10. M. De la Sen, A. Ibeas, S. Alonso-Quesada, Feedback linearization-based vaccination control strategies for true-mass action type SEIR epidemic models, *Nonlinear Anal. Model. Control*, **16**(3):283–314, 2011, https://doi.org/10.15388/NA.16.3.14094.

11. S. Metha, J. Chiasson, Nonlinear control of a series DC motor: Theory and experiment, *IEEE Trans. Ind. Electron.*, **45**(1):134–141, 1998, https://doi.org/10.1109/41.661314.

12. S. Mirjalili, A. Lewis, The whale optimization algorithm, *Adv. Eng. Software*, **83**:51–67, 2016, https://doi.org/10.1016/j.advengsoft.2016.01.008.

13. S. Mirjalili, S. M. Mirjalili, A. Lewis, Grey wolf optimizer, *Adv. Eng. Software*, **69**:46–61, 2014, https://doi.org/10.1016/j.advengsoft.2013.12.007.

14. M. Moradi, A. Ahmadi, S. Abhari, Optimal control based feedback linearization for position control of DC motor, in H. Xu (Ed.), *The 2nd IEEE International Conference on Advanced Computer Control, Shenyang, China, 27–29 March, 2010, Vol. 4*, IEEE, Piscataway, NJ, 2010, pp. 312–316, https://doi.org/10.1109/ICACC.2010.5486946.

15. M. Namazov, O. Basturk, DC motor position control using fuzzy proportional-derivative controllers with different defuzzification methods, *Turkish Journal of Fuzzy Systems*, **1**:36–54, 2010, https://www.tjfs-journal.org/TJFS_v1n1_pp36_54.pdf.

16. K. Sabahi, Application of ANN technique for DC-motor control by using FEL approaches, in J. Watada, P.-C. Chung, J.-M. Lin, C.-S. Shieh, J.-S. Pan (Eds.), *Proc. Fifth International Conference on Genetic and Evolutionary Computing, 29 August – 1 September 2011, Kinmen, Taiwan / Xiamen, China*, IEEE, Piscataway, NJ, 2011, pp. 131–134, https://doi.org/10.1109/ICGEC.2011.39.

17. S.K. Sarkar, S.K. Das, High performance nonlinear controller design for AC and DC machines: partial feedback linearization approach, *Int. J. Dyn. Control*, **6**(2):679–693, 2022, https://doi.org/10.1007/s40435-017-0330-x.

18. R. Storn, K. Price, Differential evolution-a simple and efficient heuristic for global optimization over continuous spaces, *J. Global Optim.*, **11**(4):341, 1997, https://doi.org/10.1023/A:1008202821328.

19. X. Sun, Z. Jin, Y. Cai, Z. Yang, L. Chen, Grey wolf optimization algorithm based state feedback control for a bearingless permanent magnet synchronous machine, *IEEE Trans. Power Electron.*, **35**(12):13631–13640, 2020, https://doi.org/10.1109/TPEL.2020.2994254.

20. M. Vesović, R. Jovanović, Grey wolf optimization for position control of a direct current motor driven by feedback linearization method, in M. Stanišić (Ed.), *Sinteza 2022 – International Scientific Conference on Information Technology and Data Related Research, Singidunum University, Serbia*, Singidunum Univ. Press, Belgrade, 2022, pp. 36–43, https://doi.org/10.15308/Sinteza-2022-36-43.

21. M. Vesović, R. Jovanović, L. Laban, V. Zarić, Modelling and control of a series direct current (DC) machines using feedback linearization approach, in Dejan Popović (Ed.), *Proceedings of Papers – 7th International Conference on Electrical, Electronic and Computing Engineering IcETRAN, 2020, Session AU2: Control Systems 2 AUI2.2*, Društvo za ETRAN and Akademska misao, Belgrade, Serbia, 2020, pp. 191–197, https://machinery.mas.bg.ac.rs/handle/123456789/4492.

22. M. Vesović, R. Jovanović, N. Trišović, Control of a DC motor using feedback linearization and gray wolf optimization algorithm, *Adv. Mech. Eng.*, **14**(3):16878132221085324, 2022, https://doi.org/10.1177/16878132221085324.

23. X.S. Yang, Firefly algorithms for multimodal optimization, in O. Watanabe, T. Zeugmann (Eds.), *Stochastic Algorithms: Foundations and Applications. SAGA 2009*, Lect. Notes Comput. Sci., Vol. 5792, Springer, Berlin, Heidelberg, 2009, pp. 169–178, https://doi.org/10.1007/978-3-642-04944-6_14.

24. Y. Zhang, Z. Chen, M. Sun, X. Zhang, Trajectory tracking control of a quadrotor UAV based on sliding mode active disturbance rejection control, *Nonlinear Anal. Model. Control*, **24**(4):545–560, 2019, https://doi.org/10.15388/NA.2019.4.4.